

Conformational Transition between Random Coil and Helix of Poly(*N*-propargylamides)

Jianping Deng, Junichi Tabei, Masashi Shiotsuki, Fumio Sanda, and Toshio Masuda*

Department of Polymer Chemistry, Graduate School of Engineering, Kyoto University, Kyoto 615-8510, Japan

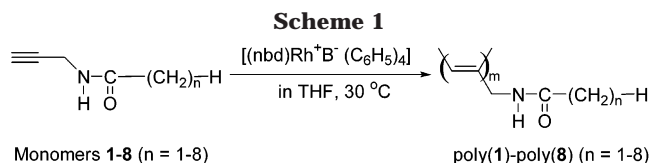
Received November 18, 2003; Revised Manuscript Received December 21, 2003

ABSTRACT: *N*-Propargylamides having pendent groups with different lengths ($\text{HC}\equiv\text{CCH}_2\text{NHCOR}$, $\text{R} = (\text{CH}_2)_n\text{H}$, $n = 1-8$) were polymerized in the presence of a Rh catalyst $[(\text{nbd})\text{Rh}^+\text{B}^-(\text{C}_6\text{H}_5)_4]$; $\text{nbd} = 2,5$ -norbornadiene] to obtain polymers with moderate molecular weight and high stereoregularity [poly(**1**)–poly(**8**)] in high yields. The conformational transition behavior of the resultant polymers was investigated by measuring UV–vis spectra in chloroform solution at different temperatures. Among the examined polymers, poly(**5**) and poly(**6**) took a stable helical conformation at relatively high temperatures, and their helical contents were the highest. Poly(**2**)–poly(**4**), which bear shorter alkyl pendent chains, did not exist in stable helical conformation owing to the lack of chain flexibility and the intermolecular hydrogen bonding. Poly(**1**) was not completely soluble in any solvents. Poly(**7**) and poly(**8**), which contain longer pendent chains, took helical conformation only at low temperatures because of the lower *cis* content of the polymer main chain. Both ΔH and ΔS for the conformational transition from random coil to helix assumed negative values, which also greatly depended on the length of the pendent groups. Whereas the helical conformation of poly(**5**) and poly(**6**) was readily generated in chloroform, neither THF nor toluene was favorable for helix formation.

Introduction

In the natural world, biomacromolecules forming the structural basis of life, such as proteins and DNA, often take helical conformations.¹ It is well-known that primary structures of the biomacromolecules assemble together by means of noncovalent forces such as hydrogen bonding, hydrophobic stacking, solvophobic effects, electrostatic interactions, and so on.² The molecular information on amino acids ranging from the sequence and hydrophilicity to the chain chirality plays a predominant role in controlling the high-order structure of the biomacromolecules. Moreover, it has been widely accepted that the conformational transition behaviors of proteins are indispensable to the activities of the living organisms. Therefore, extensive efforts have been made to investigate these characteristic behaviors of proteins.³ However, owing to the complexity of the living systems, research on the secondary structures of synthetic polymers has drawn much attention. In the meantime, progress in polymer synthesis has enabled the design and preparation of novel polymers with well-ordered helical structure, such as polyisocyanides,⁴ polyisocyanates,⁵ polychlorals,⁶ polysilanes,⁷ polyaldehydes,⁸ polymethacrylates,⁹ and polyacetylenes.^{10–13} Among them, polyacetylenes recently occupy an important position as synthetic helical polymers.

Previous research of our and other laboratories has revealed that appropriately substituted polyacetylenes can form or can be induced to form the helical structure. The driving forces are steric repulsion between bulky pendant groups^{10–12} and intramolecular hydrogen bonding between the amide groups on the side chains.¹³ In our previous studies, it has been demonstrated that a slight structural change of the pendent groups signifi-



cantly affects the stiffness of the polymer backbone, the stability of the hydrogen bond, and the stability of the helical conformation of poly(*N*-propargylamides).¹³ The present research deals with the synthesis of poly(*N*-propargylamides) bearing *n*-alkyl pendent groups with different lengths (Scheme 1) and the study of conformational transition behaviors of the formed polymers by means of variable temperature UV–vis spectroscopy, which had been proved to be a simple and effective method.^{13d} Thermodynamic parameters, e.g., ΔH and ΔS , were determined to discuss the conformational transition in detail. Further, the effects of different types of solvents on the conformational transition behavior were examined.

Experimental Section

Measurements. Melting points (mp) were measured by a Yanaco micro-melting point apparatus. ¹H and ¹³C NMR spectra were recorded on a JEOL EX-400 spectrometer. IR spectra were recorded with a Shimadzu FTIR-8100 spectrophotometer. Elemental analysis was carried out at the Kyoto University Elemental Analysis Center. Molecular weights and molecular weight distributions of the polymers were determined by GPC (Shodex KF-850 column) calibrated by using polystyrenes as standards and THF as an eluent. UV–vis spectra were recorded on a JASCO J-820 spectropolarimeter.

Materials. Solvents were distilled by the standard methods. Propargylamine (TCI), acetic acid (Aldrich), propionic acid (TCI), *n*-butyric acid (TCI), *n*-valeric acid (TCI), *n*-hexanoic acid (TCI), *n*-heptanoic acid (Wako), *n*-octanoic acid (TCI), *n*-nonanoic acid (Wako), isobutyl chloroformate (Wako), and 4-methylmorpholine (Wako) were used as received without

* Corresponding author: Tel +81-75-383-2589; Fax +81-75-383-2590; e-mail masuda@adv.polym.kyoto-u.ac.jp.

further purification. $[(\text{nbd})\text{Rh}^+\text{B}^-(\text{C}_6\text{H}_5)_4]$ was prepared as reported.¹⁴

Monomer Synthesis. All the monomers were prepared according to the literature.^{13d} Among the monomers, synthesis of monomers **1–3**, **5**, and **7** had been described earlier in detail.^{13d} The other monomers (**4**, **6**, and **8**) were prepared for the first time. Now, taking the synthesis of monomer **4** as an example, the main synthetic procedures are described. Valeric acid (5.3 mL, 49.0 mmol), isobutyl chloroformate (6.4 mL, 49.0 mmol), and 4-methylmorpholine (5.4 mL, 49.0 mmol) were added to THF (200 mL) sequentially. The solution was stirred at room temperature for about 10 min, and then propargylamine (3.4 mL, 49.0 mmol) was added to the solution. After 1 h, the white precipitate was filtered off, and the filtrate was collected, to which ethyl acetate (ca. 50 mL) was added to extract the desired product. The combined solution was washed with 2 N HCl three times and then washed with saturated aqueous NaHCO_3 to neutralize the solution. Then, the solution was dried over anhydrous MgSO_4 , filtered, and concentrated to give the target monomer. The crude monomer was further purified by flash column chromatography on silica gel (hexane/AcOEt, 2/1, v/v). Other monomers were prepared in a similar way using the corresponding carboxylic acids. The data of monomers **4**, **6**, and **8** were as follows: Monomer **4**: yield 46%, colorless crystal, mp 35–37 °C. IR (KBr): 3289 (H–N), 2928, 2361 (H–C≡), 2180, 1641 (C=O), 1545, 1469, 1277, 1118, 667, 632, 569 cm^{-1} . ^1H NMR (CDCl_3 , 400 MHz, 20 °C): δ 0.81–1.72 ($\text{CH}_2\text{C}_2\text{H}_5$), 2.22–2.31 ($\text{CH}\equiv\text{C}$, $\text{CH}_2\text{C}_2\text{H}_5$), 3.93–4.22 ($\text{CH}\equiv\text{CCH}_2$), 5.64–5.80 (NH). ^{13}C NMR (CDCl_3 , 400 MHz, 20 °C): δ 13.76, 22.34, 27.59, 29.12, 36.18, 71.50, 71.57, 172.72. Anal. Calcd for $\text{C}_8\text{H}_{13}\text{NO}$: C, 69.03; H, 9.41; N, 10.06. Found: C, 68.87; H, 9.32; N, 10.01.

Monomer **6**: yield 55%; colorless crystal, mp 72–74 °C. IR (KBr): 3292 (H–N), 2922, 2365 (H–C≡), 2182, 1637 (C=O), 1541, 669, 632, 571 cm^{-1} . ^1H NMR (CDCl_3 , 400 MHz, 20 °C): δ 0.81–1.80 ($\text{CH}_2\text{C}_4\text{H}_9$), 2.22–2.31 ($\text{CH}\equiv\text{C}$, $\text{CH}_2\text{C}_4\text{H}_9$), 3.85–4.23 ($\text{CH}\equiv\text{CCH}_2$), 5.64–5.80 (NH). ^{13}C NMR (CDCl_3 , 400 MHz, 20 °C): 14.02, 22.46, 25.48, 28.88, 29.12, 31.48, 36.47, 71.48, 71.59, 172.74. Anal. Calcd for $\text{C}_{10}\text{H}_{17}\text{NO}$: C, 71.85; H, 10.18; N, 8.38. Found: C, 71.71; H, 9.98; N, 8.41.

Monomer **8**: yield 41%; colorless crystal, mp 77–78 °C. IR (KBr): 3295 (H–N), 2924, 2366 (H–C≡), 2192, 1676 (C=O), 1550, 1275, 625, 566 cm^{-1} . ^1H NMR (CDCl_3 , 400 MHz, 20 °C): δ 0.81–1.72 ($\text{CH}_2\text{C}_6\text{H}_{13}$), 2.22–2.31 ($\text{CH}\equiv\text{C}$, $\text{CH}_2\text{C}_6\text{H}_{13}$), 3.85–4.19 ($\text{CH}\equiv\text{CCH}_2$), 5.64–5.79 (NH). ^{13}C NMR (CDCl_3 , 400 MHz, 20 °C): 14.10, 22.63, 25.54, 29.12, 29.23, 31.77, 36.49, 71.55, 76.69, 77.00, 77.31, 172.74. Anal. Calcd for $\text{C}_{12}\text{H}_{21}\text{NO}$: C, 73.85; H, 10.77; N, 7.18. Found: C, 73.72; H, 10.94; N, 7.18.

Polymerization. Polymerizations were carried out with $[(\text{nbd})\text{Rh}^+\text{B}^-(\text{C}_6\text{H}_5)_4]$ as a catalyst in dry THF at 30 °C for 1 h under the following conditions: $[\text{monomer}]_0 = 1.0 \text{ M}$, $[\text{catalyst}] = 10 \text{ mM}$. After polymerization, the resultant solution was poured into a large amount of hexane to precipitate the formed polymer. It was filtered and then dried under reduced pressure.

Results and Discussion

Polymer Synthesis. Monomers shown in Scheme 1 were polymerized with $[(\text{nbd})\text{Rh}^+\text{B}^-(\text{C}_6\text{H}_5)_4]$ catalyst, the results of which are presented in Table 1. It has been reported that the polymerization of *N*-propargylamides with Rh catalysts provides polymers with high stereoregularity, predominantly cis structure.¹⁵ This unique distinction of Rh catalysts makes them be widely employed in the polymerization of phenylacetylenes and other acetylenes in order to investigate the helical or induced circular dichroism (ICD) performance of the resultant polymers.^{10–13}

It is seen from Table 1 that all the monomers **1–8** polymerize with $[(\text{nbd})\text{Rh}^+\text{B}^-(\text{C}_6\text{H}_5)_4]$ as catalyst to give the corresponding polymers in high yields of 80% and above. Among the prepared polymers, poly(**1**) is pale

Table 1. Polymerization of *N*-Propargylamides^a

polymer	yield ^b (%)	M_n^c	M_w/M_n^c	cis content ^d (%)
poly(1)	98			
poly(2)	100	6 500	2.56	100
poly(3)	98	6 800	2.47	100
poly(4)	80	9 500	2.32	98
poly(5)	85	26 000	2.34	97
poly(6)	85	18 300	2.12	92
poly(7)	80	12 700	2.37	91
poly(8)	80	19 000	1.49	87

^a With $[(\text{nbd})\text{Rh}^+\text{B}^-(\text{C}_6\text{H}_5)_4]$ catalyst in THF at 30 °C for 1 h; $[\text{M}]_0 = 1.0 \text{ M}$; $[\text{M}]_0/[\text{Rh}] = 100$. ^b Hexane-insoluble product. ^c Measured by GPC (polystyrenes as the standard; THF as eluent).

^d Determined by ^1H NMR in CDCl_3 at 50 °C.

yellow powder, while poly(**8**) is yellow solid but more rubbery than poly(**1**); the colors of other polymers are between those of poly(**1**) and poly(**8**). In the sequence of $n = 1–8$, the polymers become more and more rubbery, indicating that the stiffness of these polymers decreases in this order. All the polymers possessed moderate molecular weights ($M_n = 6500–26\,000$), and their polydispersity indices (M_w/M_n) were in a range of ca. 1.5–2.5. Thus, it is concluded that these monomers give polymers having relatively high molecular weight in good yields.

In the ^1H NMR spectra of the resulting polymers recorded at 50 °C, the signal of the cis-olefinic proton in the main chain ($-\text{C}=\text{CH}-$) appeared around 6 ppm. By comparing the intensities of protons, the content of the cis structure was evaluated to be quite high in all these polymers. The cis contents of poly(**2**) and poly(**3**) were 100%. As the side chain became longer from poly(**1**) to poly(**8**), the cis content gradually decreased to become 87% in poly(**8**). The olefinic proton of poly(**7**) and poly(**8**) looked slightly broader than that of the other polymers. The difference of cis content observed here seems to be small, but it greatly affects the conformational transition behavior of these polymers (see below).

The solubility of the formed polymers was examined using a variety of solvents as listed in Table 2. Poly(**1**) dissolved only partly in some polar and nonpolar solvents; poly(**2**)–poly(**5**) dissolved smoothly in more solvents, but the solubility of poly(**6**)–poly(**8**) became lower again. The solubility of these polymers should be ascribed to the effect of the variation of the side chain length on the flexibility of the polymer chains.

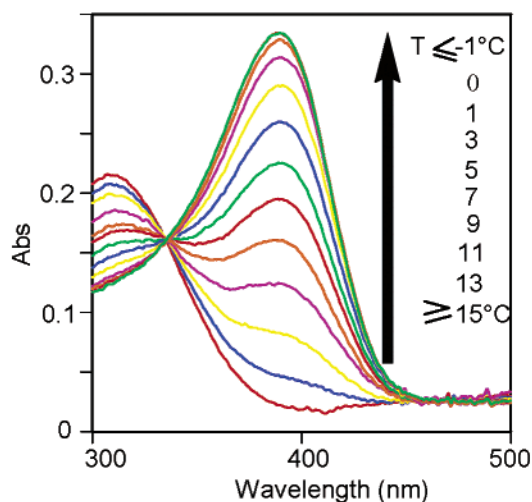
Secondary Conformation. As we have previously reported,¹³ poly(*N*-propargylamides) can be induced to form helical structure by hydrogen bonding intramolecularly occurring between the pendent amide groups. Using the polymers synthesized in the present study, the conformational transition induced by changing temperature was assessed by measuring UV–vis spectra.

In the UV–vis spectra of poly(**5**) (Figure 1), there is only one absorption peak at about 320 nm at temperature above 15 °C. In previous studies,¹³ the helical conformation of poly(*N*-propargylamides) bearing chiral groups was studied, and the relationship between the CD and UV–vis spectra of these polymers during conformational transition process was clarified. According to these studies, the polymer chain of poly(**5**) exists in random coil conformation above 15 °C. As seen in Figure 1, when the temperature was lowered to below 15 °C, a new absorption peak appeared at about 390 nm, which is ascribed to the absorption of polymer

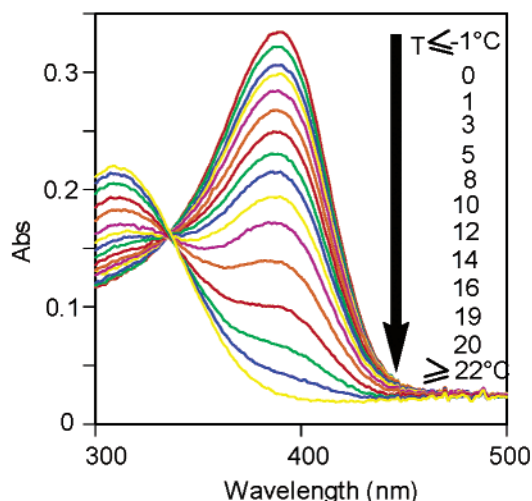
Table 2. Solubility of Poly(1)–Poly(8)^a

solvent ^b	poly(1)	poly(2)	poly(3)	poly(4)	poly(5)	poly(6)	poly(7)	poly(8)
toluene	□	□	○	○	○	○	○	○
THF	□	○	○	○	○	○	○	○
CHCl ₃	□	○	○	○	○	○	○	○
CH ₂ Cl ₂	□	□	□	□	□	□	□	□
AcOEt	×	×	□	□	□	□	×	×
acetone	□	□	□	□	□	×	×	×
DMF	□	○	○	○	□	×	×	×
DMSO	□	○	○	□	×	×	×	×
MeOH	□	○	○	○	○	□	×	×
H ₂ O	□	□	×	×	×	×	×	×

^a ○: soluble; □: partly soluble; ×: insoluble; at room temperature. ^b THF: tetrahydrofuran; AcOEt: ethyl acetate; MeOH: methanol; DMF: *N,N*-dimethylformamide; DMSO: dimethyl sulfoxide.



(a) From random coil to helix



(b) From helix to random coil

Figure 1. Temperature dependence of UV-vis spectra of poly-(5) ($c = 0.10$ mM measured in CHCl₃).

chains existing in helical structure. This indicates that the conformational transition begins around this temperature. As temperature was lowered further, the peak at 390 nm became stronger, and the peak at 320 nm became weaker simultaneously. When the temperature was lowered to -1 °C, the peak at 320 nm totally disappeared, while the peak at 390 nm became the strongest. With lowering temperature further, UV-vis spectra hardly changed. So it can be said that the helix content of the polymer leveled off at -1 °C, which can be regarded as quantitative. Thus, it is considered that the percentage of helix increases from 0 to 100% during

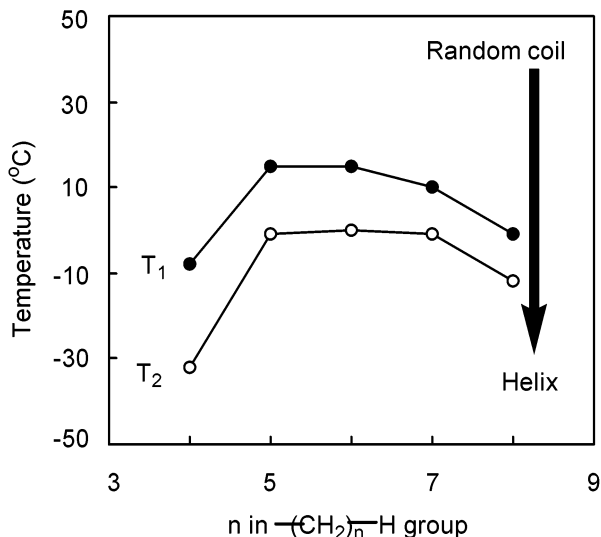
this process of random coil to helix. When temperature was raised from -1 °C, the absorption peak at 320 nm appeared again and became stronger progressively, and the intensity of the peak at 390 nm reduced simultaneously. This means that the helix percentage decreased again from 100 to 0%. Thus, it can be concluded that the conformational transition process is reversible.

Some definitions and notations of temperatures used to describe the conformational transition process in this research are as follows: The temperatures at which the conformational transition from random coil to helix begins and ends are denoted as T_1 and T_2 , respectively. The temperatures at which the conformational transition from helix to random coil begins and ends are denoted as T_3 and T_4 , respectively. The helix content at T_1 and T_3 is zero, while that at T_2 and T_4 is not necessarily 100% but takes a certain saturated value for each polymer. The T_1 – T_4 of poly(4)–poly(8) are delineated in Figure 2.

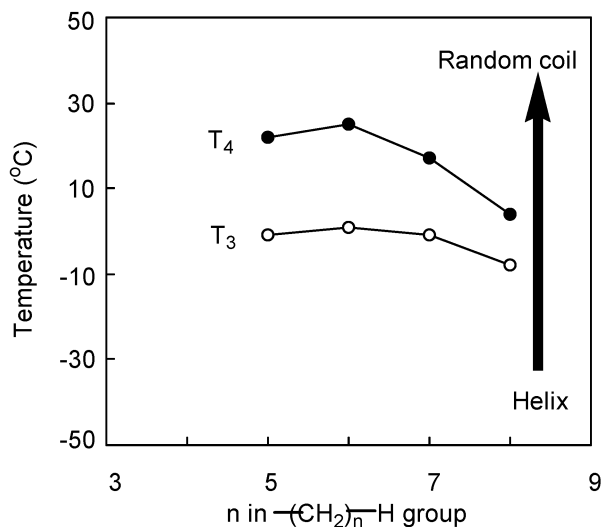
Even though temperature was decreased as low as -60 °C, the UV-vis spectra of poly(1)–poly(3) exhibited practically a single peak at around 320 nm and hardly changed. This indicates that the conformational transition of these polymers does not exist above -60 °C. Figure 2 shows that poly(5) and poly(6) can form stable helices at high temperatures. On the other hand, poly(4), poly(7), and poly(8) could take helical structure only at lower temperatures (see below for details). When the plots of T_1 and T_4 , and T_2 and T_3 , respectively, are compared, a hysteresis is observed.

As described above, poly(5) and poly(6) can form stable helices at high temperatures (Figure 2). In addition, the UV-vis absorption of poly(5) at 390 nm was the largest under the same conditions at -1 °C. Therefore, poly(5) was regarded as the standard sample, and its helix content at -1 °C was taken as 100%. In the following sections, the helix contents of the other polymers were calculated as relative values to that of poly(5).¹⁶

Figure 3 shows the helix contents of poly(2)–poly(8) at -35 °C. At this temperature all these polymers possess the saturated and highest helix contents. In the case of poly(1), which did not completely dissolve in chloroform, the conformational transition could not be examined. The UV-vis absorption spectra of poly(2) and poly(3) hardly changed, even though temperature was lowered to -60 °C. Namely, the absorption peak around 320 nm remained unchanged, and no absorption peak appeared around 390 nm. Poly(4) did not take the helical conformation unless temperature was lowered to as low as -8 °C (Figure 2), and the helix content gradually increased to become 20% at -35 °C. As mentioned above, poly(5) took helical conformation



(a) From random coil to helix



(b) From helix to random coil

Figure 2. Temperature dependence of conformational transition of poly(*N*-propargylamides). T_1 and T_2 are the temperatures at which the conformational transition from random coil to helix begins and ends, respectively; T_3 and T_4 are the temperatures at which the conformational transition from helix to random coil begins and ends, respectively.

quantitatively at -35°C . Poly(6) behaved similarly to poly(5). On the other hand, poly(7) and poly(8) exhibited a marked difference. For instance, the temperature range for the coil-to-helix transition of poly(7) was $+12$ to -1°C , while the range for the helix-to-coil transition was -1 to $+11^\circ\text{C}$; the helix content at -35°C was about 60% and not high. Further, the temperature range for the conformational transition of poly(8) from random coil to helix was $+3$ to -9°C , and that for the helix-to-coil transition was -9 to $+6^\circ\text{C}$; the helix content at -35°C was no more than about 40%.

Generally speaking, these poly(*N*-propargylamides) are flexible. In the case of polymers that are able to form stable helical conformation by means of hydrogen bonding, appropriate flexibility is important since too flexible or too stiff polymer chains are unfavorable to form strong hydrogen bonds and, in turn, stable helical conformation. It is assumed from Figures 2 and 3 that the main chain of the polymers bearing pendent groups

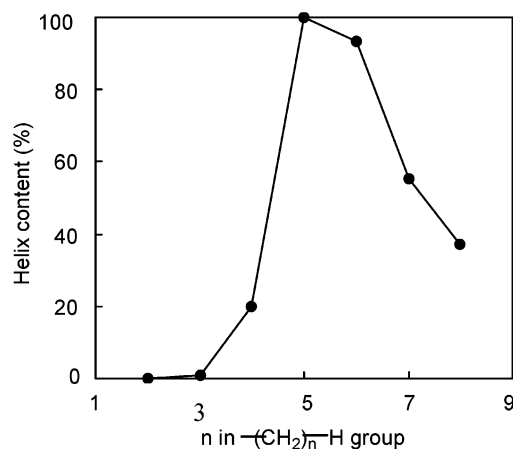


Figure 3. Helix content of poly(*N*-propargylamides) with various alkyl lengths determined by UV-vis spectroscopy measured in CHCl_3 ($c = 0.10$ mM) at -35°C .

with appropriate length [poly(5) and poly(6)] becomes sufficiently flexible, and simultaneously intramolecular hydrogen bonding occurs effectively. As a consequence, their conformational transition should take place at relatively high temperatures, and their helical structure should be sufficiently stable.

When the length of the pendent groups is too short [poly(1)–poly(4)], two points should be taken into account. First, intermolecular hydrogen bonding but not intramolecular hydrogen bonding seems to be formed again due to the short pendent alkyl groups. Second, the flexibility of the polymer backbones is insufficient because of the shorter pendent alkyl groups. Both of these two points are unfavorable for the polymers to take helical conformation. Regarding the hydrogen bonding, the following experiments were designed and carried out: The UV-vis spectra of poly(3) were recorded with different concentrations. It was observed that when the concentration was decreased from 0.1 to 0.05 mM, a weak absorption peak appeared at 390 nm below -42°C , the intensity of which became slightly stronger upon further decrease of temperature ($\geq -60^\circ\text{C}$). When the concentration was lowered further, e.g., to 0.025 mM, the UV-vis spectroscopic pattern showed nearly the same as that of 0.05 mM, but the molar absorptivity at 390 nm became slightly larger than that of 0.05 mM. It is suggested on the basis of these phenomena that an appreciable amount of intermolecular hydrogen bonding is formed, which has negative effects on the formation of helical conformation.

In the case of polymers bearing longer pendent groups such as poly(7) and poly(8), even though the polymers became more flexible than poly(5) and poly(6), the longer pendent groups exerted negative effects on the stereoregularity of the polymer main chain, as discussed in the polymer synthesis part. It is likely that stereoregularity is one of the essential factors for the poly(*N*-propargylamide) chain to take ordered helical structure. Therefore, it is reasonable to consider that the decrease of *cis* content resulted in lower stability of the induced helical structure of poly(7) and poly(8).

To understand more clearly the characteristics of conformational transition behavior of these polymers, we calculated thermodynamic parameters, i.e., ΔH (change in enthalpy) and ΔS (change in entropy) for the coil-to-helix transition. According to the van't Hoff equation, $\Delta G = -RT \ln K = \Delta H - T\Delta S$, which describes the relationship between equilibrium constant ($\ln K$)

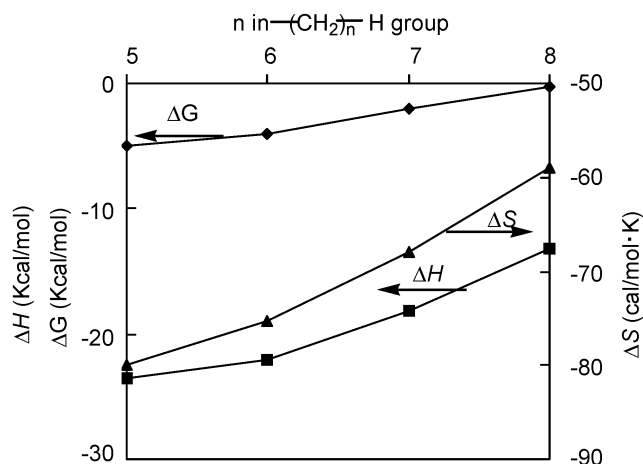


Figure 4. Thermodynamic parameters for the coil-to-helix transition of poly(*N*-propargylamides) with various alkyl lengths. The ΔG values are the ones calculated for -35 °C.

and absolute temperature (T), where ΔH and ΔS can be determined from the plot of $\ln K$ against $1/T$. This plot is based on the equation $\ln K = -\Delta H/RT + \Delta S/R$, where ΔG is the change in free energy, K the equilibrium constant of the coil-to-helix transition and equal to N_h/N_r (N_h and N_r are the monomer units existing in helix and random coil, respectively), and R the gas constant. Figure 4 plots the ΔH and ΔS values against n of $(\text{CH}_2)_n\text{-H}$ group in poly(*N*-propargylamides). As seen from Figure 4, when the helical conformation is less stable as in poly(7) and poly(8), both ΔH and ΔS give smaller values with negative sign; in contrast, poly(5) and poly(6), which have stable helical conformation, give larger values with negative sign for both ΔH and ΔS .

From the viewpoint of entropy, the conformational transition from random coil to helix is unfavorable, especially with polymers like poly(*N*-propargylamides) having flexible main chains. Namely, the coil-to-helix transition leads to a drastic decrease of entropy. However, the decrease of entropy can be offset by the decrease of enthalpy, which is explained in terms of the stabilization of helix formation based on hydrogen bonding. Therefore, in the case of poly(7) and poly(8), the unstable helical conformation just caused a small decrease of entropy and enthalpy, while larger values with negative sign were observed for both entropy and enthalpy in poly(5) and poly(6) which form more stable helical conformation. These reasonings are proved by the values of ΔG in Figure 4. ΔG became larger in the sequence of poly(8), poly(7), poly(6), and poly(5) with negative sign, providing evidence for reasoning that poly(5) and poly(6) form more stable helices than poly(7) and poly(8) do.

Solvent Effects. In general, solvents more or less exhibit influence on the secondary structure of polymer chains. In this study, almost all the UV-vis spectra were recorded using chloroform as solvent because it is a good solvent for poly(*N*-propargylamides), has a moderate polarity, and hardly participates in hydrogen bonding.

To elucidate the effect of solvents on the transition process, poly(5) and poly(6) were employed as samples, and THF and toluene were used as solvents apart from chloroform. It was confirmed that no conformational transition was observed even though temperature was lowered as low as -60 °C in these two solvents under

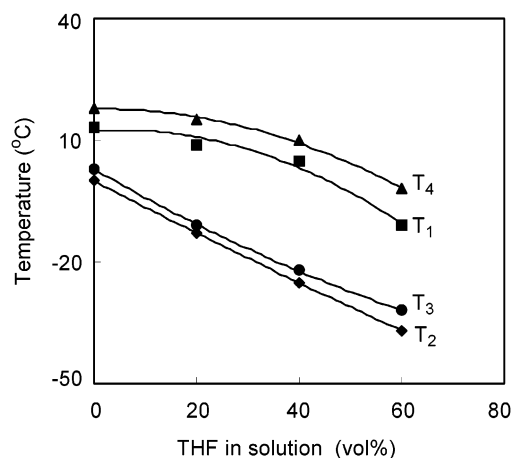


Figure 5. Effect of THF on the transition temperatures T_1 – T_4 in the poly(5)/ CHCl_3 system ($c = 0.10$ mM). T_1 and T_2 are the temperatures at which the coil-to-helix transition begins and ends, respectively; T_3 and T_4 are the temperatures at which the helix-to-coil transition begins and ends, respectively.

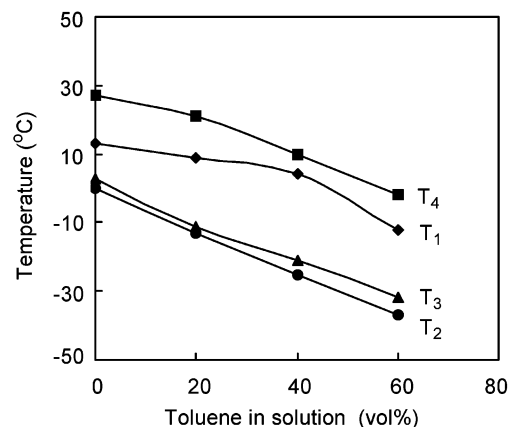


Figure 6. Effect of toluene on transition temperatures T_1 – T_4 in the poly(6)/ CHCl_3 system ($c = 0.10$ mM). See Figure 5 for the definition of T_1 – T_4 .

the same conditions as for chloroform. The reason is probably that THF can form hydrogen bonding with the amide group on the pendent chain of the polymer. In toluene solution, on the other hand, there is a significant difference in polarity between the polymer chain and toluene, especially pendent chains and the solvent. Consequently, the polymer chains will not fully extend and hence will mainly exist in the form of tight coil, and in turn, hydrogen bonding will hardly take place.

Addition of various amounts of THF or toluene to polymer/chloroform systems provided interesting results as presented in Figures 5 and 6. The definitions of T_1 , T_2 , T_3 , and T_4 in Figures 5 and 6 are the same as those in Figure 2. The temperature dependence of the conformational transition from random coil to helix or from helix to random coil was also observed clearly when different amounts of THF or toluene were added to the polymer solution. As seen in Figure 5, by adding THF to the poly(5)/chloroform system, all of the transition temperatures (T_1 – T_4) more or less decreased compared with those in the absence of THF (THF = 0 mL), reflecting the effect of THF on the conformational transition behavior. The THF molecule bears an oxygen atom, so that hydrogen bonding is predominantly formed between the oxygen atom of THF and $-\text{NH}-$ of the amide group of polymer chains, which results in breaking of the hydrogen bonding formed between $-\text{NH}-$ and

–CO– groups in the pendent amide group of the polymer. Consequently, it should be more difficult for the polymer chains to take helical conformation as THF increases.

Results similar to those in Figure 5 were observed in the poly(**6**)/chloroform system containing different amounts of toluene (Figure 6). With increasing amount of toluene in the poly(**6**)/chloroform system, all the transition temperatures T_1 – T_4 gradually decreased. This is probably because it became more difficult for the polymer chains to take an extended flexible conformation which can lead to helical structure.

Conclusions

The conformational transition of poly(*N*-propargylamides) bearing pendent groups with various lengths was examined in detail. The length of the pendent groups exhibited significant effects on the stereoregularity of the polymer main chain, the stiffness of the polymer backbone, and the solubility of the polymers. Consequently, the pendent groups greatly affected the conformational transition behavior of the polymers, including the temperature range in which the polymer chains to take helical structure and the helix contents. Increasing the length of the pendent groups was favorable to enhance the flexibility of the polymers, but in the meantime, it caused a decrease in stereoregularity of the polymer main chain. The former was helpful for the conformational transition from random coil to helical structure, but the latter exerted adverse effects on it. In the same way, shortening the length of the pendent groups increased the stereoregularity of the polymer backbones and presumably resulted in the formation of not only intra- but intermolecular hydrogen bonding as well. Therefore, it is difficult for the polymers bearing too short or too long pendent groups to take stable helical conformation, and consequently, poly(**5**) and poly(**6**) formed stable helices even at relatively high temperature. Solvents exhibited significant effects on the secondary conformation of the polymers. Among the three solvents, chloroform, THF, and toluene, chloroform was the most suitable for the polymer chains to take helical conformation.

References and Notes

- (1) (a) Saenger, W. *Principles of Nucleic Acid Structure*; Springer-Verlag: New York, 1984. (b) Schula, G. E.; Schirmer, R. H. *Principles of Protein Structure*; Springer-Verlag: New York, 1979.
- (2) Ofagail, C. *Stabilizing Protein Function*; Springer-Verlag: Hong Kong, 1997.
- (3) (a) Baldwin, R. L.; Rose, G. D. *Trends Biochem. Sci.* **1999**, *24*, 26–33. (b) Dobson, C. M.; Sali, A.; Karplus, M. *Angew. Chem., Int. Ed.* **1998**, *37*, 868–893. (c) Brenner, S.; Chothia, C.; Hubbard, T. J. P. *Curr. Opin. Struct. Biol.* **1997**, *7*, 369–376. (d) Matthews, B. M. *Methods Enzymol.* **1997**, *276*, 3–10.
- (4) (a) Ito, Y.; Ohara, T.; Shima, R.; Sugimoto, M. *J. Am. Chem. Soc.* **1996**, *118*, 9188–9189. (b) Takei, F.; Yanai, K.; Onitsuka, K.; Takahashi, S. *Angew. Chem., Int. Ed. Engl.* **1996**, *35*, 1554–1555.
- (5) (a) Jha, S. K.; Cheon, K. S.; Green, M. M.; Selinger, J. V. *J. Am. Chem. Soc.* **1999**, *121*, 1665–1673. (b) Okamoto, Y.; Matsuda, M.; Nakano, T.; Yashima, E. *J. Polym. Sci., Part A: Polym. Chem.* **1994**, *32*, 309–315.
- (6) Ute, K.; Hirose, K.; Kashimoto, H.; Hatada, K.; Vogel, O. J. *Am. Chem. Soc.* **1991**, *113*, 6305–6306.
- (7) (a) Nakashima, H.; Fujiki, M.; Koe, J. R. *Macromolecules* **1999**, *32*, 7707–7709. (b) Fujiki, M. *J. Am. Chem. Soc.* **1994**, *116*, 11976–11981.
- (8) Choi, S.-H.; Yashima, E.; Okamoto, Y. *Macromolecules* **1996**, *29*, 1880–1885.
- (9) (a) Nakano, T.; Okamoto, Y. *Chem. Rev.* **2001**, *101*, 4013–4038. (b) Okamoto, Y.; Nakano, T. *Chem. Rev.* **1994**, *94*, 349–372. (c) Okamoto, Y.; Suzuki, K.; Ohta, K.; Hatada, K.; Yuki, H. *J. Am. Chem. Soc.* **1979**, *101*, 4763–4765.
- (10) (a) Nonokawa, R.; Oobo, M.; Yashima, E. *Macromolecules* **2003**, *36*, 6599–6606. (b) Maeda, K.; Goto, H.; Yashima, E. *Macromolecules* **2001**, *34*, 1160–1164. (c) Maeda, K.; Okada, S.; Yashima, E.; Okamoto, Y. *J. Polym. Sci., Part A: Polym. Chem.* **2001**, *39*, 3180–3189. (d) Saito, M. A.; Maeda, K.; Onouchi, H.; Yashima, E. *Macromolecules* **2000**, *33*, 4616–4618.
- (11) (a) Li, B. S.; Cheuk, K. K. L.; Ling, L.; Chen, J.; Xiao, X.; Bai, C.; Tang, B. Z. *Macromolecules* **2003**, *36*, 77–85. (b) Li, B. S.; Cheuk, K. K. L.; Salhi, F.; Lam, J. W. Y.; Cha, J. A. K.; Bai, C. L.; Tang, B. Z. *Nano Lett.* **2001**, *1*, 323–328.
- (12) (a) Nakako, H.; Nomura, R.; Tabata, M.; Masuda, T. *Macromolecules* **2001**, *34*, 1496–1502. (b) Nomura, R.; Fukushima, Y.; Nakako, H.; Masuda, T. *J. Am. Chem. Soc.* **2000**, *37*, 8830–8831. (c) Nakako, H.; Mayahara, Y.; Nomura, R.; Tabata, M.; Masuda, T. *Macromolecules* **2000**, *33*, 3978–3982. (d) Nakako, H.; Nomura, R.; Tabata, M.; Masuda, T. *Macromolecules* **1999**, *32*, 2861–2864.
- (13) (a) Nomura, R.; Nishiura, S.; Tabei, J.; Sanda, F.; Masuda, T. *Macromolecules* **2003**, *36*, 5076–5080. (b) Nomura, R.; Tabei, J.; Nishiura, S.; Masuda, T. *Macromolecules* **2003**, *36*, 561–564. (c) Tabei, J.; Nomura, R.; Masuda, T. *Macromolecules* **2002**, *35*, 5405–5409. (d) Nomura, R.; Tabei, J.; Masuda, T. *Macromolecules* **2002**, *35*, 2955–2961. (e) Nomura, R.; Tabei, J.; Masuda, T. *J. Am. Chem. Soc.* **2001**, *123*, 8430–8431.
- (14) Richard, R. S.; Osborn, J. A. *Inorg. Chem.* **1970**, *10*, 2339–2343.
- (15) (a) Tabata, M.; Sone, T.; Sadahiro, Y. *Macromol. Chem. Phys.* **1999**, *200*, 265–268. (b) Masuda, T. In *Catalysis in Precision Polymerization*; Kobayashi, S., Ed.; Wiley: Chichester, 1997; Chapter 2.4.
- (16) The helix contents of polymers were calculated as follows: Poly(**6**) is taken as an example. The highest UV–vis absorption intensities of poly(**5**) (at –1 °C) and poly(**6**) (at 0 °C) at 390 nm are defined as $A_{390\text{ nm}}$ and $B_{390\text{ nm}}$, respectively; the UV–vis absorption intensities of poly(**5**) and poly(**6**) at the isosbestic point are denoted as $C_{390\text{ nm}}$ and $D_{390\text{ nm}}$, respectively. Then the helix content of poly(**6**) is determined by the following equation: helix content (%) = $(B_{390\text{ nm}}D_{390\text{ nm}})/(A_{390\text{ nm}}C_{390\text{ nm}}) \times 100$.

MA035735D